Magnetic state of EuN: X-ray magnetic circular dichroism at the Eu $M_{4,5}$ and $L_{2,3}$ absorption edges

B. J. Ruck,[1] H. J. Trodahl,[1] J. H. Richter,[1] J. C. Cezar,[2] F. Wilhelm,[2] A. Rogalev,[2] V. N. Antonov,[3] Binh Do Le,[1] and C. Meyer[4]

[1]*The MacDiarmid Institute for Advanced Materials and Nanotechnology, School of Chemical and Physical Sciences, Victoria University, Wellington 6140, New Zealand*

[2]*European Synchrotron Radiation Facility, Boîte Postale 220, F-38043 Grenoble CEDEX, France*

[3]*Institute of Metal Physics, National Academy of Sciences of Ukraine, 03142 Kiev, Ukraine*

[4]*Institut Néel, Centre National de la Recherche Scientifique and Université Joseph Fourier, B.P. 166, F-38042 Grenoble Cedex, France*

(Received 3 March 2011; revised manuscript received 21 March 2011; published 2 May 2011)

We report $M_{4,5}$- and $L_{2,3}$-edge x-ray magnetic circular dichroism (XMCD) studies of the ion-specific magnetic polarization on Eu in europium mononitride. The absorption spectra at both edges show a main signal originating from Eu^{3+} with a well-separated small ($\sim 2\%$) contribution from a Eu^{2+} valence state that we propose is associated with a small concentration of N vacancies. Magnetic polarization is observed in both $4f$ and $5d$ orbitals and for both valence states. The temperature and field dependence of the $M_{4,5}$-edge XMCD signal shows a van Vleck signature from Eu^{3+} (main EuN contribution) and a Brillouin paramagnetic signal from the small concentration of Eu^{2+} ions. In addition, the $L_{2,3}$ edge shows that the Eu^{3+} ions have $5d$ orbitals that are polarized both by intra-ion f-d exchange and by inter-ionic d-d exchange from neighboring Eu^{2+} ions. There is no evidence of magnetic order among the Eu ions at temperatures as low as 10 K.

DOI: 10.1103/PhysRevB.83.174404 PACS number(s): 75.50.Pp, 75.30.Cr, 78.70.Dm, 71.28.+d

I. INTRODUCTION

The rare-earth mononitrides adopt the NaCl structure, among the simplest structures available as testing grounds for the effects of exchange among their strongly localized $4f$ levels. They have been investigated experimentally since the 1960s,[1–3] although it is only relatively recently that they have begun to yield to efforts to avoid N deficiency and O contamination. The picture of electronic structures that emerges from the few that have been extensively studied is of predominantly narrow-gap semiconductor[4–9] or semimetal[10] (YbN) band structures. In view of their weak conductivity, both N vacancies of order 1% and O contamination can severely affect the measured value, but such low-density defects have a weaker effect on the magnetic properties, so that for the most part their ferromagnetic ground states were firmly established 40 years ago.[1,2] There are two notable exceptions: (i) SmN was originally suspected to be antiferromagnetic and (ii) to date there appears to be only one very old magnetic study of EuN, only at temperatures above 300 K and on samples with more than 6% oxygen contamination.[3] In the case of SmN, we established that it is ferromagnetic below 27 K, but with a moment of only $0.03\mu_B$ per formula unit resulting from a near cancellation of the $4f$ spin and orbital moments on the Sm^{3+} ions,[11] but the low-temperature magnetic state of EuN is still uncertain. In this paper we investigate the Eu M- and L-edge x-ray magnetic circular dichroism (XMCD) signatures in epitaxial films of EuN. We find a weak van Vleck signal from Eu^{3+} and, at low temperatures, a conventional paramagnetic signal from $\sim 2\%$ Eu^{2+}, but no evidence of magnetic order at any temperature of 10 K or above.

Despite the scarcity of experimental data, EuN has attracted the attention of theorists. There exist several band-structure calculations based on density-functional theory (DFT), most of which show overlapping valence and conduction bands and predict metallic conduction with a relatively small carrier density.[12–17] As expected, for their ionic bonding and in common with the other rare-earth nitrides, the valence band is of N $2p$ and the conduction band of Eu $5d$ character. Eu is in the trivalent state and an empty majority $4f$ level lies very close to the bottom of the conduction band. A Eu^{2+} configuration that is only slightly more energetic has also been reported.[14]

The magnetic state of EuN has also been discussed from a theoretical perspective.[16] The zero total angular momentum ($J = 0$) of Eu^{3+} in its ground state prevents any moment alignment without some $J = 1$ and higher admixture. It is clear that such an admixture can be driven by an external field, as is the basis of the van Vleck paramagnetic response. The question then arises as to whether any $J > 0$ admixture might spawn magnetic order in EuN, though to our knowledge there are no known Eu^{3+} materials that display magnetic order. However, even within the zero-J constraint it is suggested that a strong interatomic exchange may drive a strong spin correlation, possibly even with a diverging correlation length at some characteristic temperature.[16] With rigorously zero total angular momentum, the correlations will not be signaled in susceptibility measurements. In order to initiate an investigation of these possibilities, we study the magnetic response of epitaxial EuN films.

Work is in progress growing and passivating EuN films.[18] To date, we have measured moderate resistivities (0.5–10 mΩ cm) and a positive temperature coefficient of resistivity (TCR), typical of either a heavily doped semiconductor or a semimetal, but with no clear signal of an activated conductivity that would clearly establish that EuN is a semiconductor. In common with GdN,[5,7] we expect the films to have a moderate concentration of N vacancies that act as donors and dope the films n type. A recent local spin-density approximation (LSDA) + U (where U is the effective on-site Coulomb repulsion) calculation for GdN has shown that nitrogen vacancies have a formation energy of order 0.5 eV,[19] which could explain N vacancies (V_N) of order 1% at the $>600\,^{\circ}$C temperature required for epitaxial growth. To date, the V_N formation energy in EuN is unknown, but it is likely that vacancies at the 1% level would dope even a semiconductor to degeneracy and lead to a

positive TCR. It should be noted, however, that the presence of an unoccupied $4f$ band near the conduction band of EuN emphasizes the potential for a donated electron to bind to a neighboring Eu^{3+} ion, thus forming divalent or mixed-valent Eu ions. From the experimental perspective any study of the magnetic response of Eu^{3+} compounds is susceptible to contamination by Eu^{2+}. The expected van Vleck response of Eu^{3+} ions is weak, so that the enormous $7\mu_B$ moment on the $J = 7/2$ Eu^{2+} ion dominates at least the low-temperature magnetic response for even a small Eu^{2+} concentration.[20]

II. EXPERIMENTAL DETAILS

The x-ray spectroscopy in this study was performed on epitaxial EuN films grown by pulsed laser deposition (PLD) onto the (100) face of yttrium-stabilized zirconia (YSZ), while simultaneously exposing the substrate to nitrogen from a plasma source. After completing the growth, the films were capped *in situ* with YSZ. These substrates and caps have a large parasitic magnetic signal, so for superconducting quantum interference device (SQUID) studies we used AlN-passivated, (111)-oriented epitaxial films grown on a (0001) AlN buffer layer in turn grown on (0001) sapphire, as has been successful for GdN growth.[21] The film growth was monitored by reflection high-energy electron diffraction (RHEED) and subsequent *ex situ* x-ray diffraction (XRD) confirmed their orientation.

SQUID measurements were performed on films grown to a thickness of 110 nm at 0.02 nm/sec onto a substrate held at $\sim 650\,^{\circ}$C. Despite the weak substrate signal, it still dominates the magnetic response. The signal from the thin film is weaker by almost two orders of magnitude and on the limit of measurability. After subtracting the substrate signal, there remains the expected van Vleck paramagnetic signal of approximately 6×10^{-3} emu/mol (Refs. 20 and 22) and at the lowest temperatures an additional paramagnetic signal [$(0.02 \pm 0.01$ K emu/mol)/T], suggesting a low concentration ($\sim 2.5\%$) of Eu ions in the divalent state. These net-moment measurements are compromised by the uncertainty introduced by the substrate and by the mixed Eu^{3+}-Eu^{2+} response, immediately suggesting an investigation exploiting the valence- and orbital-selective resolution of XMCD. It will be seen that those x-ray spectroscopic data show direct evidence for just such a low concentration of Eu^{2+}.

X-ray-absorption spectroscopy (XAS) and XMCD measurements were performed at the Eu $M_{4,5}$ and $L_{2,3}$ edges on the ID08 and ID12 beam lines at the European Synchrotron Radiation Facility in Grenoble. The spectral distortion from fluorescent photon self-absorption at $\sim 10^3$ eV dictated that total electron yield (TEY) was used as a measure of absorption at the M edge. Furthermore, the M-edge signal was strongly attenuated by absorption in the capping layer and the signal-to-noise ratio was then limited by noise in the inelastic background TEY signal from the cap. Much weaker absorption of the ~ 7-KeV x rays at the L edge permitted recording of distortion- and noise-free spectra using the total fluorescence yield detection mode.

Eu $M_{4,5}$-edge ($3d^{10}4f^6 \rightarrow 3d^9 4f^7$ in Eu^{3+}, $3d^{10}4f^7 \rightarrow 3d^9 4f^8$ in Eu^{2+}) XAS involves changes in occupation of the closely localized $4f$ orbitals and thus is only weakly dependent on the bonding configuration. It will be seen in the data that the XMCD spectra are easily separated into contributions from Eu^{2+} and Eu^{3+} ions, permitting the independent exploration of the magnetic behavior of these two ionic species. In contrast, the $L_{2,3}$-edge ($2p^6 5d^0 \rightarrow 2p^5 5d^1$) XAS and XMCD interrogate the more extended $5d$ empty-state orbitals, and interpretation of these require guidance from modeling that includes band-structure effects. We discuss these in Sec. III.

III. CALCULATED $L_{2,3}$-EDGE XAS AND XMCD

Computational methods described previously[23,24] have been applied to calculate the expected L-edge spectra of EuN in the face-centered-cubic structure of sodium chloride, using the spin-polarized fully relativistic linear muffin-tin orbital (LMTO) method,[25,26] with the combined correction term taken into account. We used the Perdew-Wang[27] parametrization for the exchange correlation potential. Brillouin zone integrations were performed using the improved tetrahedron method[28] and the charge was obtained self-consistently with 349 irreducible **k** points. To improve the potential we included additional empty spheres. The basis consisted of Eu s, p, d, and f; N s, p, and d; and empty spheres s and p LMTOs. The effect of an external magnetic field on the band structure can be accounted for by including in the Hamiltonian the sum of the Zeeman term

$$H_Z = \mu_B \mathbf{B} \cdot (\hat{\mathbf{l}} + 2\hat{\mathbf{s}}), \tag{1}$$

which couples spin $\hat{\mathbf{s}}$ and orbital $\hat{\mathbf{l}}$ moments of an electron to the external magnetic field **B**. In the present work, the band structure of EuN in an external magnetic field was calculated self-consistently with the matrix elements of the Zeeman term (1) included to the Hamiltonian matrix of the LMTO method at the variational step. The intrinsic broadening mechanisms have been accounted for by folding the XMCD spectra with a Lorentzian. For the finite lifetime of the core hole, a constant width Γ_c in general form[29] has been used. The finite resolution of the spectrometer has been accounted for by a Gaussian of 0.6 eV.

The application of plain LSDA calculations to $4f$-electron systems is often inappropriate because of the correlated nature of the $4f$ shell.[30] The position of the LSDA $4f$ states close to the Fermi energy contradicts x-ray photoemission spectroscopy (XPS), ultraviolet photoemission spectroscopy (UPS), and x-ray spectroscopy data.[30–32] For improved treatment of the on-site f-electron correlations, we have adopted as a suitable model the LSDA + U approach, using the rotationally invariant LSDA + U method.[33,34] The effective on-site Coulomb repulsion U was treated as an adjustable parameter; ultimately 7 eV was chosen. For the exchange integral $\mathcal{J}$ the value of 0.66 eV was estimated from constrained LSDA calculations.

The energy-band structure of EuN was calculated in the LSDA + U approximation for the trivalent nonmagnetic Eu^{3+} (configuration $4f^6$) and divalent magnetic Eu^{2+} (configuration $4f^7$) ions. In order to imitate the nonmagnetic ($J = 0$) ground state of the Eu^{3+} ion the exchange-correlation potential is taken to be the same for both spin states within the corresponding atomic spheres. The six $4f_{5/2}$ Eu^{3+} bands are fully occupied and situated in the gap between the nitrogen $2s$ and $2p$ states

while eight $4f_{7/2}$ hole levels are completely unoccupied and cross the bottom of the unoccupied Eu $5d$ band. For divalent ferromagnetic Eu ions the seven $4f$ spin-up fully occupied energy bands cross the bottom of N $2p$ valence-band states situated around 0.9–1.9 eV below the valence-band maximum. The other seven $4f$ spin-down divalent Eu energy bands are situated far above the Fermi level at 8.5–9.8 eV and are strongly hybridized with Eu $5d$ states.

The XMCD spectra at the Eu $L_{2,3}$ edges are mostly determined by the strength of the spin-orbit (SO) coupling of the initial Eu $2p$ core states and spin polarization of the final empty $5d_{3/2,5/2}$ states, while the exchange splitting of the Eu $2p$ core states, as well as the SO coupling of the $5d$ valence states, are of minor importance for the XMCD at the Eu $L_{2,3}$ edges of EuN. Note that the Eu $5d$ states in EuN have band character and extend over more than 13 eV, so that calculations based on density-functional theory may be expected to give a good description of the Eu XAS and XMCD spectra at the $L_{2,3}$ edge.

We investigated the core-hole effect in the final state, checking the convergence of XAS and XMCD spectra for the impurity site. We used supercell calculations with two and four formula units in the case of EuN. At one of the two or four Eu atoms, we create a hole at the $2p_{1/2}$ or $2p_{3/2}$ levels for the self-consistent calculations of the L_2 and L_3 spectra, respectively. The spectra for two and four formula units was found to be very similar. We found only a minor influence of the final-state interaction on the shape of the Eu $L_{2,3}$ XMCD spectra across the entire energy interval.

IV. RESULTS AND DISCUSSIONS

The Eu $M_{4,5}$-edge XAS data (Fig. 1) show an overwhelming preponderance of Eu^{3+}, though, in agreement with XPS and SQUID results, there is a small ($\approx 3\%$) concentration of Eu^{2+} indicated by the weak feature near 1132 eV.[35] In contrast, the XMCD spectrum in Fig. 2 is dominated by a feature at that energy for the lowest temperatures, signaling the dominant magnetic role played by even this small concentration of Eu^{2+} ions. The weaker signal that remains to dominate at higher

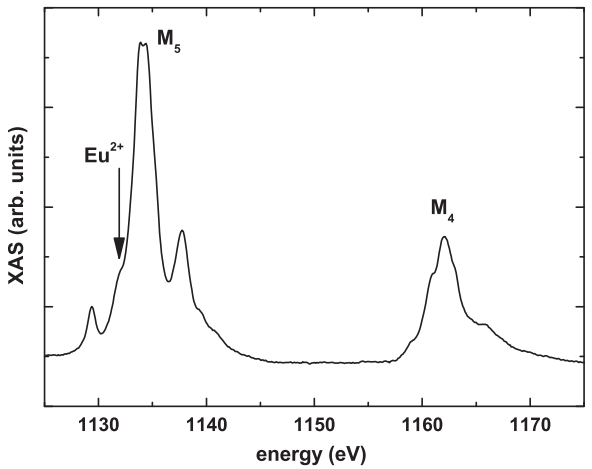

FIG. 1. XAS at the Eu $M_{4,5}$ edges in EuN. The shoulder at 1132 eV is due to a small concentration of Eu^{2+} ions, probably adjacent to N vacancies.

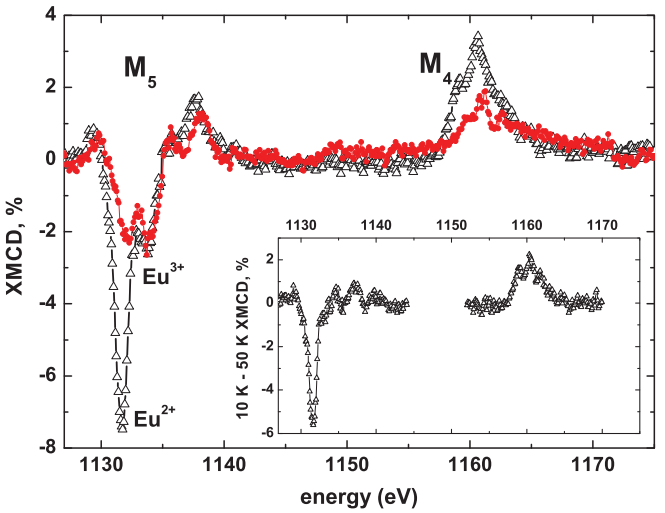

FIG. 2. (Color online) Eu $M_{4,5}$-edge XMCD spectra of EuN measured in a field of 5 T: black open triangles, 10 K spectra; red closed circles, 50 K spectra. The peaks at 1132 and 1134 eV arise from Eu^{2+} and Eu^{3+} ions, respectively. The inset is the difference between the 10- and 50-K spectra, and represents the signal from the small concentration of Eu^{2+} ions.

temperatures relates to the $J = 1$ excited state of Eu^{3+} and is a direct signature of the van Vleck paramagnetic response. The van Vleck admixture shows no significant temperature dependence below 100 K,[20,22] so that the difference between the 10- and 50-K spectra in Fig. 2 can be regarded as a purely Eu^{2+} spectrum as shown in the inset. The zero integral of the difference spectrum across the two edges confirms its source as the $L = 0$ ground state of Eu^{2+}.[36] Its amplitude with rising temperature follows the paramagnetic Brillouin function for $J = 7/2$ and a moment of $7\mu_B$ (Fig. 3).The Eu^{3+} amplitude is also shown in the figure. It is temperature independent within its uncertainty. There is no hysteresis (not shown) in either signal, confirming the SQUID results that neither the Eu^{2+} nor

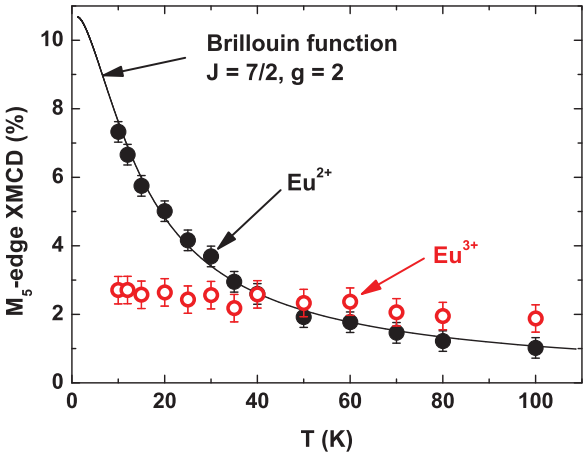

FIG. 3. (Color online) Eu M_5-edge amplitudes at 1131 eV (black filled circles) and 1134 eV (open red circles) are measures of the moments on the Eu^{2+} and Eu^{3+} ions, respectively. The black line is a fit to the Eu^{2+} moment by the Brillouin function appropriate for a half-filled $4f$ shell in a field of 5 T.

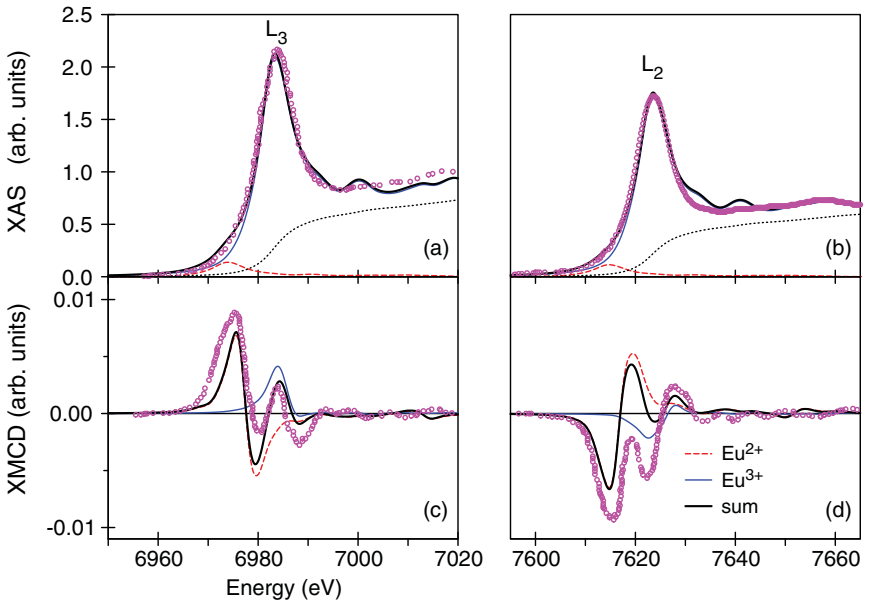

FIG. 4. (Color online) Experimental x-ray-absorption spectra (circles) of EuN at the Eu (a) L_3 and (b) L_2 edges, respectively, in comparison with the theoretically calculated spectra in the LSDA + U approach: dashed red lines present the x-ray absorption from the magnetic Eu^{2+} ions, full blue lines are from nonmagnetic Eu^{3+} ions, dotted lines show the theoretically calculated background spectra, and full thick black lines are the sum of the theoretical Eu^{2+}, Eu^{3+}, and background spectra. Experimental XMCD spectra (circles) of EuN at the Eu (c) L_3 and (d) L_2 edges, respectively, in comparison with theoretically calculated spectra in the LSDA + U approximation: dashed red lines present the XMCD spectra from the magnetic Eu^{2+} ions, full blue lines are from nonmagnetic Eu^{3+} ions, and full thick black lines are the sum of the theoretical Eu^{2+} and Eu^{3+} spectra.

the Eu^{3+} ions participate in a magnetically ordered state at temperatures of 10 K or higher.

We turn next to the $L_{2,3}$-edge XAS and XMCD data taken at 10 K in a field of 5 T, compared in Fig. 4 to the calculated spectra in the LSDA + U approximation. The x-ray-absorption spectra at both the L_3 and L_2 edges consist of a single major peak for each charge state. However, the XMCD spectra are rather complicated. The L_3 edge has two positive peaks and two negative peaks. The L_2 edge has two negative peaks and one positive peak. Fitting the XAS spectra again requires a few percent of divalent Eu, creating tiny shoulders at 6974 and 7614 eV on the L_3 and L_2 edges, respectively. However, even such a small concentration of Eu^{2+} ions contributes to strong XMCD signals [red dashed curves in Fig. 4(c) and 4(d)].

Although Eu^{3+} ions in the $J = 0$ state would produce zero x-ray dichroism, the van Vleck admixture of $J = 1$ in an external magnetic field leads to an XMCD signal that is both seen in the data and reproduced in the calculation. As can be seen from Fig. 4(c), the first two low-energy peaks at the L_3 edge, one maximum and one minimum, are mostly determined by contributions from magnetic Eu^{2+} ions, while the next two peaks at 6984 and 6989 eV are due to field-polarized Eu^{3+} ions. A similar situation also occurs at the L_2 edge [see Fig. 4(d)], with both the divalent and trivalent signals showing a minimum followed by a maximum, though here there is strong overlap between the second divalent and the first trivalent signals. We make corrections for this overlap in our interpretation of the temperature-dependent spectra below.

The measured XMCD spectral patterns show agreement with theoretical simulated spectra after adjustment of the divalent-trivalent ratio, but disagreements remain in the details, such as the relative intensities of the various features. It is important to note that the Eu^{2+} calculations treat fully periodic crystals in which every Eu site has the same valence. In contrast, the EuN film has a relatively dilute concentration of Eu^{2+} ions in a crystal with predominantly trivalent ions, which may explain the different spectral details.

In order to investigate the temperature dependence, Fig. 5 displays the L_2-edge XMCD spectra from 10 to 110 K. The feature at 7615 eV, which is clearly associated with divalent ions, loses intensity with rising temperature, in agreement with the analogous feature on the M_5 edge; it follows the $5d$ polarization on Eu^{2+} ions. Conversely, the deep minimum at 7622 eV is predominantly driven by a negative peak from the trivalent ions, with a smaller opposing positive contribution from divalent ions. This 7622-eV, predominantly Eu^{3+}, feature shows reduced intensity with increasing temperature, in direct contrast to the temperature-independent Eu^{3+} $4f$-derived signal in the M-edge XMCD. The temperature dependence clearly signals a spin polarization in $5d$ orbitals on Eu^{3+} ions neighboring divalent ions. As seen in Fig. 4(d), the calculated Eu^{2+} signal at 7622 eV is approximately 30% of the value at the 7615.5-eV feature (and of the opposite sign). Thus we treat [XMCD(7622 eV) + 0.3 XMCD(7615.5 eV)] as a measure of the Eu^{3+} $5d$ polarization and plot it in Fig. 6 against the Eu^{2+} $5d$ polarization as measured by the 7615.5-eV XMCD amplitude. The linear dependence demonstrates a

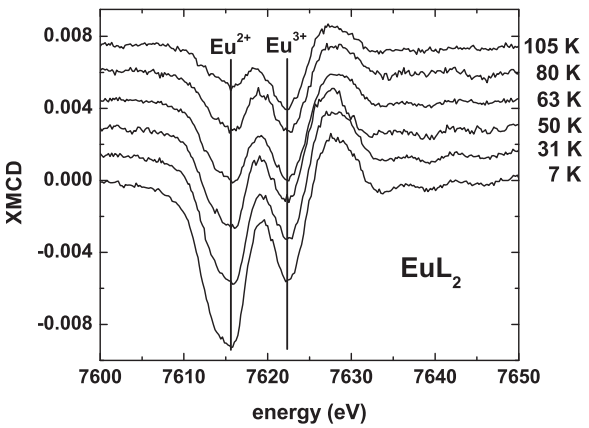

FIG. 5. Eu L_2 spectra at various temperatures between 7 and 105 K. The amplitude of the negative peak at 7615.5 eV arises from the small concentration of Eu^{2+} ions, while the amplitude at 7622 eV has contributions from a negative Eu^{3+} peak and a positive Eu^{2+} signal (see Fig. 4).

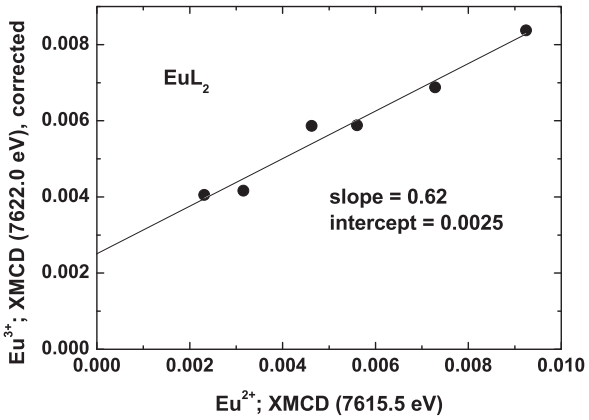

FIG. 6. Eu^{3+} L_2 signal at 7622 eV, corrected for a small Eu^{2+} contribution, plotted vs the Eu^{2+} amplitude. The temperatures vary between 7 K for the largest signal at the right to 100 K for the smallest signals at the left.

strong Eu^{2+}-driven polarization of Eu^{3+} ions; the average Eu^{3+} $5d$ polarization below 10 K is more than doubled by the inter-ion d-d exchange from neighboring Eu^{2+} ions. The Eu^{3+} $5d$ signal remaining at higher temperatures arises from intra-ion f-d exchange and a van Vleck susceptibility in the $4f$ orbitals.

Recalling that the L-edge XMCD spectra reflect the $5d$ polarization, the data indicate that an excess $5d$ polarization on Eu^{3+} ions is induced by polarized Eu^{2+} in the network and it is in the same sense as the polarization determined by the ferromagnetic intra-ionic f-d exchange on the Eu^{3+} ion itself. Not surprisingly, that d-orbital polarization is too weak to develop any $J = 1$ admixture on the Eu^{3+} ions, as is demonstrated by the lack of a temperature dependence in the trivalent XMCD signal at the M edge. Nonetheless, the ferromagnetic alignment of the $5d$ orbitals might polarize a neighboring Eu^{2+} ion and one might speculate that the EuN system will thus develop DMS-like ferromagnetic behavior at sufficiently high divalent ion concentration. The question arises as to how close another divalent ion would need to be in order for that transferred polarization to provide a sufficient Eu^{2+}-Eu^{2+} exchange to develop bulk ferromagnetism.

V. CONCLUSIONS

We have reported XAS and XMCD spectra from both the $M_{4,5}$ and the $L_{2,3}$ edges of Eu in EuN, probing the empty $4f$ and $5d$ orbitals, respectively. The XAS spectra show N vacancies at the level of 1–3 %, likely related to the low V_N formation energy. XMCD on the two edges permits an investigation of orbital- ($4f$,$5d$) and valence- (Eu^{3+},Eu^{2+}) specific magnetic moments on Eu ions in the network. $M_{4,5}$-edge spectra show clearly that the $7\mu_B$ moments on Eu^{2+} $4f$ orbitals are uncorrelated, following the expected Brillouin function and behaving as independent Curie-law moments to at least 10 K, while the $4f$ moments on Eu^{3+} ions show only the temperature independence (up to 100 K) from a van Vleck paramagnetic response. $L_{2,3}$ XMCD shows that the $5d$ orbitals on Eu^{2+} ions follow the Curie-law response, in complete agreement with the Eu^{2+} $4f$ polarization, exactly as expected in the presence of intra-ionic f-d exchange. In contrast, the Eu^{3+} $5d$ orbitals polarize as a mixture of the van Vleck response driven by on-site f-d exchange, supplemented by a Curie-law response driven by inter-ionic d-d exchange between Eu^{2+} ions and their Eu^{3+} neighbors. The latter suggests that the material might form a dilute magnetic semiconductor at sufficiently high divalent ion concentration.

ACKNOWLEDGMENTS

We are grateful for expert assistance in film growth from Franck Natali and Ian Farrell. The research was supported by the New Zealand New Economy Research Fund, Grant No. VICX0808, and the Marsden Fund, Grant No. 08-VUW-030. The MacDiarmid Institute is supported by the New Zealand Centres of Research Excellence Fund.

[1] F. Hulliger, *Handbook on the Physics and Chemistry of Rare Earths* (North-Holland Physics, New York, 1978), Vol. 4, pp. 153–236.

[2] O. Vogt and K. Mattenberger, *Handbook on the Physics and Chemistry of Rare Earths* (Elsevier, Amsterdam, 1993), Vol. 17, pp. 301–407.

[3] R. Didchenko and F. P. Gortsema, J. Phys. Chem. Solids **24**, 863 (1963).

[4] F. Leuenberger, A. Parge, W. Felsch, K. Fauth, and M. Hessler, Phys. Rev. B **72**, 014427 (2005).

[5] S. Granville, B. J. Ruck, F. Budde, A. Koo, D. J. Pringle, F. Kuchler, A. R. H. Preston, D. H. Housden, N. Lund, A. Bittar, G. V. M. Williams, and H. J. Trodahl, Phys. Rev. B **73**, 235335 (2006).

[6] A. R. H. Preston, S. Granville, D. H. Housden, B. Ludbrook, B. J. Ruck, H. J. Trodahl, A. Bittar, G. V. M. Williams, J. E. Downes, A. DeMasi, Y. Zhang, K. E. Smith, and W. R. L. Lambrecht, Phys. Rev. B **76**, 245120 (2007).

[7] M. A. Scarpulla, C. S. Gallinat, S. Mack, J. S. Speck, and A. C. Gossard, J. Cryst. Growth **311**, 1239 (2009).

[8] H. J. Trodahl, A. R. H. Preston, J. Zhong, B. J. Ruck, N. M. Strickland, C. Mitra, and W. R. L. Lambrecht, Phys. Rev. B **76**, 085211 (2007).

[9] C. Meyer, B. J. Ruck, A. R. H. Preston, S. Granville, G. V. M. Williams, and H. J. Trodahl, J. Magn. Magn. Mater. **322**, 1973 (2010).

[10] L. Degiorgi, W. Bacsa, and P. Wachter, Phys. Rev. B **42**, 530 (1990).

[11] C. Meyer, B. J. Ruck, J. Zhong, S. Granville, A. R. H. Preston, G. V. M. Williams, and H. J. Trodahl, Phys. Rev. B **78**, 174406 (2008).

[12] M. Horne, P. Strange, W. M. Temmerman, Z. Szotek, A. Svane, and H. Winter, J. Phys. Condens. Matter **16**, 5061 (2004).

[13] C. M. Aerts, P. Strange, M. Horne, W. M. Temmerman, Z. Szotek, and A. Svane, Phys. Rev. B **69**, 045115 (2004).

[14]P. Larson, W. R. L. Lambrecht, A. Chantis, and M. van Schilfgaarde, Phys. Rev. B **75**, 045114 (2007).
[15]C.-G. Duan, R. F. Sabirianov, W. N. Mei, P. A. Dowben, S. S. Jaswal, and E. Y. Tsymbal, J. Phys. Condens. Matter **19**, 315220 (2007).
[16]M. D. Johannes and W. E. Pickett, Phys. Rev. B **72**, 195116 (2005).
[17]L. Petit, R. Tyer, Z. Szotek, W. M. Temmerman, and A. Svane, New J. Phys. **12**, 113041 (2010).
[18]J. Richter, B. J. Ruck, and M. Simpson (unpublished).
[19]A. Punya, T. Cheiwchanchamnangij, A. Thiess, and W. R. L. Lambrecht, *MRS Online Proceedings Library*, Vol. 1290, mrsf10-1290-i04-04 (2011).
[20]Y. Takikawa, S. Ebisu, and S. Nagata, J. Phys. Chem. Solids **71**, 1592 (2010).
[21]F. Natali, N. O. V. Plank, J. Galipaud, B. J. Ruck, H. J. Trodahl, F. Semond, S. Sorieul, and L. Hirsch, J. Cryst. Growth **312**, 3583 (2010).
[22]J. H. Van Vleck, *The Theory of Electric and Magnetic Susceptibilities* (Oxford University Press, Oxford, 1932).
[23]V. N. Antonov, H. A. Dürr, Y. Kucherenko, L. V. Bekenov, and A. N. Yaresko, Phys. Rev. B **72**, 054441 (2005).
[24]V. N. Antonov, A. P. Shpak, and A. N. Yaresko, Low Temp. Phys. **34**, 79 (2008).
[25]O. K. Andersen, Phys. Rev. B **12**, 3060 (1975).
[26]V. V. Nemoshkalenko, A. E. Krasovskii, V. N. Antonov Vl, N. Antonov, U. Fleck, H. Wonn, and P. Ziesche, Phys. Status Solidi B **120**, 283 (1983).
[27]J. P. Perdew and Y. Wang, Phys. Rev. B **45**, 13244 (1992).
[28]P. E. Blöchl, O. Jepsen, and O. K. Andersen, Phys. Rev. B **49**, 16223 (1994).
[29]J. C. Fuggle and J. E. Inglesfield, *Unoccupied Electronic States, Topics in Applied Physics* (Springer, New York, 1992), Vol. 69.
[30]V. N. Antonov, B. Harmon, and A. N. Yaresko, *Electronic Structure and Magneto-Optical Properties of Solids* (Kluwer, Dordrecht, 2004).
[31]P. Wachter, *Handbook on the Physics and Chemistry of Rare Earths* (North-Holland Physics, Amsterdam, 1994), Vol. 19, p. 177.
[32]A. R. H. Preston, B. J. Ruck, W. R. L. Lambrecht, L. F. J. Piper, J. E. Downes, K. E. Smith, and H. J. Trodahl, Appl. Phys. Lett. **96**, 032101 (2010).
[33]V. I. Anisimov, J. Zaanen, and O. K. Andersen, Phys. Rev. B **44**, 943 (1991).
[34]A. N. Yaresko, V. N. Antonov, and P. Fulde, Phys. Rev. B **67**, 155103 (2003).
[35]B. T. Thole, G. van der Laan, J. C. Fuggle, G. A. Sawatzky, R. C. Karnatak, and J.-M. Esteva, Phys. Rev. B **32**, 5107 (1985).
[36]B. T. Thole, P. Carra, F. Sette, and G. van der Laan, Phys. Rev. Lett. **68**, 1943 (1992).